

High electron mobility W-doped In_2O_3 thin films by pulsed laser deposition

P. F. Newhouse, C.-H. Park, and D. A. Keszler

Department of Chemistry, Oregon State University, Corvallis, Oregon 97331-4003

J. Tate^{a)}

Department of Physics, Oregon State University, Corvallis, Oregon 97331-6507

P. S. Nyholm

Hewlett-Packard Company, 1000 NE Circle Boulevard, Corvallis, Oregon 97330-4239

(Received 22 April 2005; accepted 8 August 2005; published online 9 September 2005)

High electron mobility thin films of $\text{In}_{2-x}\text{W}_x\text{O}_{3+y}$ ($0 \leq x \leq 0.075$) were prepared on amorphous SiO_2 and single-crystal yttria-stabilized zirconia (001) substrates by pulsed laser deposition. Mobilities ranged between 66 and 112 cm^2/Vs depending on the substrate type and deposition conditions, and the highest mobility was observed at a W-dopant concentration of $x \sim 0.03$. A small band gap shift was detected from films with increasing electron carrier density; the electron effective mass calculated from Burstein-Moss theory was $0.3m_e$. $\text{In}_{2-x}\text{W}_x\text{O}_{3+y}$ films have high visible transmittance of $\sim 80\%$. © 2005 American Institute of Physics. [DOI: 10.1063/1.2048829]

Refractory metal doping of In_2O_3 has been explored using Ta, Mo, Zr, Ti, or even codoping with Mo and W.¹⁻³ These reports have been received with enthusiasm as they have shown that transparent thin films exhibiting exceptional carrier mobility μ can be prepared if Mo is chosen as the dopant. In particular, evaporated⁴ thin films of $\text{In}_2\text{O}_3:\text{Mo}$ (IMO) on glass substrates have exhibited $\mu \sim 130 \text{ cm}^2/\text{Vs}$ with electrical conductivity σ of $\sim 5900 \text{ S/cm}$.³ Sputtered⁵ and laser ablated⁶ IMO films have demonstrated best-case mobilities of 83 cm^2/Vs on glass and $>95 \text{ cm}^2/\text{Vs}$ on yttria-stabilized zirconia (YSZ), respectively. These values are factors of 2–3 greater than those measured in commercial grade⁶ $\text{In}_2\text{O}_3:\text{Sn}$ (ITO; $\sigma = 5000 \text{ S/cm}$, $n = 6.6 \times 10^{20} \text{ cm}^{-3}$, $\mu = 47 \text{ cm}^2/\text{Vs}$) and research grade⁷ $\text{In}_2\text{O}_3:\text{Sn}$ ($\sigma \sim 13\,000 \text{ S/cm}$, $n = 1.9 \times 10^{21} \text{ cm}^{-3}$, $\mu = 42 \text{ cm}^2/\text{Vs}$). Sputtered undoped² In_2O_3 films and those doped with Ta,¹ Zr, or Ti, exhibit mobilities smaller than IMO, typically about 30 cm^2/Vs . Here we report transport, structure, and compositional measurements on W-doped In_2O_3 thin films (IWO) fabricated by pulsed laser deposition. We show that W is an effective dopant for realizing a high mobility transparent conducting oxide (TCO). These high mobilities are found in polycrystalline films with small dopant concentrations and are prepared at moderate temperatures on amorphous substrates. This is significant because increasing the carrier mobility is the preferred route to optimizing the electrical conductivity, thereby averting transparency losses from free-carrier absorption.⁸

Thin films of $\text{In}_{2-x}\text{W}_x\text{O}_{3+y}$ were deposited onto heated GE 124 fused SiO_2 and single-crystal YSZ (001) substrates using pulsed laser ablation of ceramic $\text{In}_2\text{O}_3:\text{WO}_3$ pellets in a UHV chamber with a base pressure of 2×10^{-9} torr. Targets of about 60% of theoretical density were prepared by solid-state synthesis from stoichiometric proportions of In_2O_3 and WO_3 with $x_{\text{target}} = 0, 0.025, 0.0375, 0.05, 0.0625$, and 0.075. The targets, polished prior to each use, were ablated in pure O_2 ambient by pulsed radiation from KrF excimer laser operating at 10 Hz and $\sim 0.5 \text{ J/cm}^2$. Ambient pressure during deposition was typically a few millitorr. The

target was 45 mm from the substrate, and both were rotated during the deposition to enhance ablation and deposition uniformity. Deposition rates for the 0.3–0.5 μm thick films were about 0.1 nm/pulse. The substrate was maintained at a constant temperature between 400°C and 525°C during the deposition. After deposition, the films cooled to below 70 °C in the oxygen ambient.

Films were characterized by x-ray diffraction (XRD), electrical conductivity, Hall-effect measurements, electron probe microanalysis (EPMA), and by optical transmission and reflection. XRD spectra were measured with a Rigaku Rapid R-axis diffractometer at fixed incident angle with specimen rotation. Electrical conductivity and Hall mobility were measured on cross-shaped samples in the van der Pauw configuration on a Lakeshore 7704 Hall measurement at room temperature and $\sim 77 \text{ K}$. EPMA was performed using a Cameca SX50 electron microprobe using multivoltage thin-film analysis (15, 20, and 25 kV, at each of five different film locations). Optical transmission and reflection spectra in the UV-visible range were measured using a double-grating spectrometer with a Xe lamp source and a Si diode detector.

Figure 1 shows the results of room-temperature (solid diamonds) and 77-K (open diamonds) transport measurements as a function of film doping level as determined by EPMA for a series of IWO films prepared on fused SiO_2 substrates under the same deposition conditions (1 mtorr O_2 , 400 °C, 0.5 J/cm^2). Optimized room-temperature transport properties of $\mu = 66 \text{ cm}^2/\text{Vs}$, $\sigma = 3.1 \times 10^3 \text{ S/cm}$, $n = 2.90 \times 10^{20} \text{ cm}^{-3}$, were found when $x_{\text{film}} \sim 0.03$. Increasing the oxygen pressure to 4 mtorr (solid circle) increased the mobility to close to 80 cm^2/Vs . Increasing the substrate temperature to 525 °C (triangle) significantly improved the room-temperature mobility and conductivity ($\mu = 104 \text{ cm}^2/\text{Vs}$, $\sigma = 3.3 \times 10^3 \text{ S/cm}$), and the equivalent film on a YSZ (001) single-crystal substrate (cross) showed $\mu = 112 \text{ cm}^2/\text{Vs}$ and $\sigma = 4.5 \times 10^3 \text{ S/cm}$, representing the best-case room-temperature transport results in this study.

Transport measurements at 77 K on all films in the diamond series showed the same general trends as the room-temperature measurements. The mobility and conductivity increase up to $x \sim 0.03$ followed by a steady decrease at

^{a)}Electronic mail: tate@physics.orst.edu

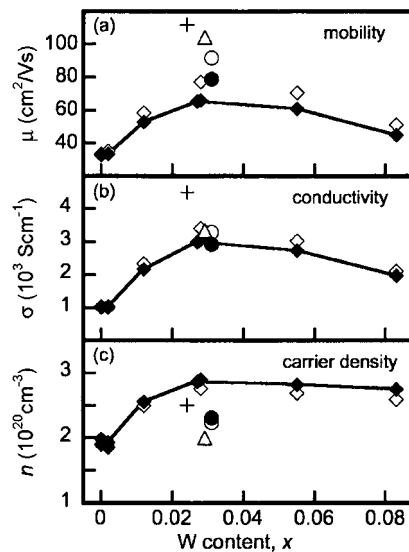


FIG. 1. Room temperature and ~ 77 K (a) Hall mobility, (b) conductivity, and (c) carrier density for several IWO films prepared on fused SiO_2 and single-crystal YSZ (001) substrates. The symbols are explained in the text. The lines are a guide.

higher dopant concentration. The elevated mobility at low temperature is consistent with decreased phonon scattering. For films of high dopant concentration, scattering by ionized impurities is also significant as evidenced by the falloff in mobility at both low and high temperatures.

The carrier density for the diamond series of films remains essentially constant when $x_{\text{film}} \geq 0.03$, following an initial increase in the carrier density when $x_{\text{film}} < 0.03$ due to incorporation of W into the host lattice. The low-temperature carrier density is only slightly decreased, indicating that the carriers are not thermally activated over this temperature range. In principle, W^{6+} substitution on In^{3+} sites in In_2O_3 could generate as many as three electron carriers per W. However, this level of doping efficiency has not been observed in this or closely related systems like IMO.⁶ For the highest carrier concentration IWO films, the doping efficiency is < 0.75 electrons/W, suggesting that W substitutes in a lower valent configuration.

Determination of the W content of the IWO films is crucial. EPMA provides a reliable quantitative measure of film composition provided careful attention is paid to eliminating substrate interference and to the variation of excitation volume with incident-beam energy.⁹ In this work, background corrections for each element were carefully applied to avoid interference from any overlapping or satellite lines. The detection limit for W was at worst 0.15 wt %, which corresponds to $x = 0.0023$. The averaged k -ratio data corrected for dead time, background, and drift were refined in STRATAGEM,¹⁰ a thin-film composition software program that performs a matrix correction to account for sample geometry and substrate.

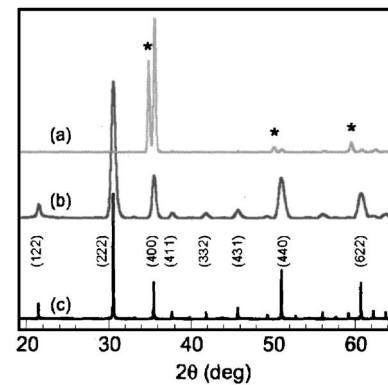


FIG. 2. XRD patterns for textured IWO films on (001) YSZ (a), polycrystalline IWO films on fused SiO_2 (b), and calculated for undoped In_2O_3 (c). Asterisks mark the position of YSZ reflections.

The EPMA results are summarized in Table I. The W concentration of the film deviates significantly from that of the target, especially for low doping levels. The high mobility IWO films prepared from targets of W doping level $x_{\text{target}} = 0.05$ using 0.5 J/cm^2 have a dopant concentration of $x_{\text{film}} = 0.028$. This result was reproducible for many films prepared from the same target, irrespective of substrate temperature or background gas pressure. Films prepared from targets with $x_{\text{target}} = 0.025$ using 0.5 J/cm^2 showed only trace amounts of W by EPMA and their mobility was also characteristic of undoped In_2O_3 . However, by increasing the incident laser fluence to 2 J/cm^2 , high mobility films could be prepared from $x = 0.025$ targets. This indicated that some amount of W was transferred to the film in the ablation plume at this higher fluence, and EPMA showed that the W content of these high mobility films was significant at $x_{\text{film}} = 0.016$. Overall, x_{film} determination by EPMA provided a more consistent interpretation of the variation of transport properties with dopant concentration. It is likely that the observed nonstoichiometric transfer of W from the $\text{In}_2\text{O}_3:\text{WO}_3$ targets resulted from the use of low laser energy density and from low target density, which can further dilute the incident laser fluence by increasing the effective surface area of the irradiated region.¹¹ The low-density targets also imposed practical limitations on the incident laser fluence due to severe pitting of the target surface at higher fluence. Using targets of higher density will permit the proper investigation of this key deposition parameter.

Figure 2 shows the XRD patterns for IWO films deposited on fused SiO_2 and YSZ (001) at substrate temperatures of 400 and 525 °C, respectively. A calculated XRD pattern for undoped In_2O_3 is shown in Fig. 2(c).¹² Both films can be indexed completely to In_2O_3 . The amorphous background due to the fused SiO_2 has been subtracted from Fig. 2(b), and in Fig. 2(a) asterisks mark the positions of YSZ substrate reflections. The film on SiO_2 is polycrystalline, while the

TABLE I. Nominal x_{target} doping level for $\text{In}_2\text{O}_3:\text{WO}_3$ targets and resultant x_{film} as determined by EPMA for 0.5 and 2 J/cm^2 incident laser fluence.

Fluence (J/cm^2)	0.5	0.5	0.5	0.5	0.5	0.5	2
x_{target}	0	0.025	0.0375	0.05	0.0625	0.075	0.025
x_{film}	0	0.002	0.012	0.028	0.055	0.083	0.016

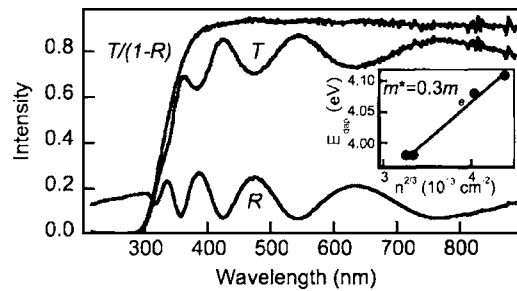


FIG. 3. Optical transmission T , reflection R , and reflection-corrected transmission $T/(1-R)$ for a 0.3- μm IWO film on a fused SiO_2 substrate. Inset: Burstein-Moss shift illustrated by E_g vs $n^{2/3}$.

film on the YSZ single-crystal substrate shows (00 l) preferential orientation.

Figure 3(a) shows the UV-visible transmission T , reflection R , and reflection-corrected transmission $T/(1-R) \approx e^{-\alpha d}$ for a typical IWO film-substrate stack. Here d is the film thickness and α the absorption coefficient. The average raw transparency is about 80%, a value representative of most films produced in this work. Thickness values obtained from fitting a calculated R to the experimentally obtained spectrum agree within 5% with values obtained via mechanical profilometry, and the refractive index ($n=1.99$ at 500 nm) is close to published values¹³ for ITO thin films. The direct band gap was obtained from plots of $(\alpha h\nu)^2$ versus $h\nu$ and extrapolating to the $h\nu=0$ axis, from which it was found that E_g varied between about 3.80 and 3.91 eV for most films.

The Burstein-Moss shift, in which the onset of transmission in the films is pushed into the UV as the carrier density increases,^{14,15} is observed in the transmission spectra. The widening of the band gap is given by¹⁶

$$\Delta E_g^{BM} = \frac{\hbar^2}{2m^*} (3\pi^2 n)^{2/3}, \quad (1)$$

where n is the carrier density and m^* is the reduced effective mass. The plot of E_g versus $n^{2/3}$ (inset of Fig. 3) gives $m^* = 0.3m_e$, in good agreement with values for ITO¹⁶ and IMO.⁵

There has been no theoretical description of the mechanism leading to exceptional carrier mobility in IMO and IWO thin films. However, Yoshida *et al.* have found that the carrier effective mass in high mobility IMO thin films remains constant over a range of carrier concentrations while the scattering time is maximized for films with the optimum doping level of 2 wt % Mo ($\text{In}_{1.94}\text{Mo}_{0.06}\text{O}_{3+y}$) and $n=3.0 \times 10^{20} \text{ cm}^{-3}$. Hence, high mobility IMO films result from decreased scattering, rather than decreased carrier effective mass.⁵

W-doped films show significantly higher mobility than undoped In_2O_3 films, which could indicate that W assists in

suppression of scattering by oxygen interstitials. This mechanism has been posited for Mo-doped films.⁵ W itself may become a dominant scattering center above $x_{\text{film}} \sim 0.03$, as indicated by the mobility decrease in Fig. 1(a). Also, EPMA data of IWO films suggests that W might be a more efficient dopant than Mo for the suppression of scattering by oxygen interstitials, since mobility in the IMO system is optimal when $x=0.06$ ($\text{In}_{1.94}\text{Mo}_{0.06}\text{O}_{3+y}$) (Ref. 6), while in the IWO system mobility is maximized when $x_{\text{film}} \sim 0.03$.

We have prepared high electron mobility thin films of transparent conductor $\text{In}_{2-x}\text{W}_x\text{O}_{3+y}$ on fused SiO_2 and single-crystal YSZ (001) substrates by pulsed laser deposition. The highest mobility and conductivity was measured for films with $x \sim 0.03$, and room-temperature mobilities as large as 104 and 112 cm^2/Vs could be realized on fused SiO_2 and YSZ substrates, respectively. Low-temperature Hall-effect measurements on high mobility IWO films indicate that the electron mobility is constrained by phonon scattering and ionized impurity scattering. A widening of the band gap with increasing electron density was observed, from which an electron effective mass of $0.3m_e$ was obtained.

We thank John Donovan of CAMCOR at the University of Oregon for assistance with EPMA, and Tim Murrell and Susan Guyler for help with the transport and optical measurements. This material is based on work supported by the National Science Foundation under Grant No. 0245386 and by Hewlett-Packard Company.

¹H. Ju, S. Hwang, C. Jeong, C. Park, E. Jeong, and S. Park, J. Korean Phys. Soc. **44**, 956 (2004).

²Y. Yoshida, C. Warmstrong, T. A. Gessert, J. D. Perkins, D. S. Ginley, and T. J. Coutts, Mater. Res. Soc. Symp. Proc. **747**, 207 (2003).

³Y. Abe, U.S. Patent No. 20040013899 (pending).

⁴Y. Meng, X. Yang, H. Chen, J. Shen, Y. Jiang, Z. Zhang, and Z. Hua, Thin Solid Films **394**, 219 (2001).

⁵Y. Yoshida, D. Wood, T. A. Gessert, and T. J. Coutts, Appl. Phys. Lett. **84**, 2097 (2004).

⁶C. Warmstrong, Y. Yoshida, D. W. Readey, C. W. Teplin, J. D. Perkins, P. A. Parilla, L. M. Gedvilas, B. M. Keyes, and D. S. Ginley, J. Appl. Phys. **95**, 3831 (2004).

⁷H. Ohta, M. Orita, M. Hirano, H. Tanji, H. Kawazoe, and H. Hosono, Appl. Phys. Lett. **76**, 2740 (2000).

⁸T. J. Coutts, D. L. Young, and X. Li, Mater. Res. Soc. Symp. Proc. **623**, 199 (2000).

⁹J. L. Pouchou and F. Pichoir, Scanning **12**, 212 (1990).

¹⁰STRATAGEM 3.0 Thickness and Compositional Thin Film Analysis Package, (SAMx, Saint Andre de la Roche, France, 1997).

¹¹Pulsed Laser Deposition of Thin Films, edited by D. B. Chrisey and G. K. Hubler (Wiley, New York, 1994) pp. 106-107.

¹²JCPDS Powder Diffraction File, No. 71-2195 (1997).

¹³S. Laux, N. Kaiser, A. Zoller, R. Gotzelmann, H. Lauth, and H. Bernitzki, Thin Solid Films **335**, 1 (1998).

¹⁴E. Burstein, Phys. Rev. **93**, 632 (1954).

¹⁵T. S. Moss, Proc. Phys. Soc. London **B67**, 775 (1954).

¹⁶I. Hamberg and C. G. Granqvist, J. Appl. Phys. **60**, R123 (1986).